AQ STEM CELLS AND DEVELOPMENT XX:1–8 (2008)

DOI: 10.1089/scd.2007.0197

Neuronal Differentiation Potential of Human Adipose-Derived Mesenchymal Stem Cells

Elena Anghileri,[1,*] Silvia Marconi,[1,*] Angela Pignatelli,[2] Pierangelo Cifelli,[2] Mirco Galié,[3] Andrea Sbarbati,[3] Mauro Krampera,[4] Ottorino Belluzzi,[2] and Bruno Bonetti[1]

Adult mesenchymal stem cells derived from adipose tissue (A-MSC) have the capacity to differentiate in vitro into mesenchymal as well as endodermal and ectodermal cell lineages. We investigated the neuronal differentiation potential of human A-MSC with a protocol which included sphere formation and sequential culture in brain-derived neurotrophic factor (BDNF) and retinoic acid (RA). After 30 days, about 57% A-MSC showed morphological, immunocytochemical and electrophysiological evidence of initial neuronal differentiation. In fact, A-MSC displayed elongated shape with protrusion of two or three cellular processes, selectively expressed nestin and neuronal molecules (including GABA receptor and tyroxine hydroxilase) in the absence of glial phenotypic markers. Differentiated cells showed negative membrane potential (−60 mV), delayed rectifier potassium currents and TTX-sensitive sodium currents. Such changes were stable for at least 7 days after removal of differentiation medium. In view of these results and the easy availability of adipose tissue, A-MSC may be a ready source of adult MSC with neuronal differentiation potential, an useful tool to treat neurodegenerative diseases.

Introduction

Mesenchymal stem cells (MSC) are elements with multi-differentiation potential isolated from bone marrow (BM) (1) and from other sources, including the adipose tissue (2, 3). In addition to their ability to differentiate into osteoblasts, adipocytes and chondrocytes (4), BM-MSC display also neuro-ectodermic (5, 6) and endodermic differentiation potential (7, 8). Neural differentiation has been achieved with different experimental protocols using chemical agents, growth factors or co-cultures with neural cells. In general, chemical agents induced transient morphological changes with general up-regulation of several neural markers (9–12), growth factors promoted more specific and prolonged neural modification (8, 13, 14), while complete neuronal differentiation has been obtained only after co-culture with astroglial or neuronal cells (5, 15, 16). Most of these studies on the neural differentiation of MSC have been performed on BM-MSC, while few information are available for MSC obtained from other sources. Adipose-derived MSC (A-MSC) may represent a valid alternative to BM-MSC, because of their pluripotency and ability to differentiate in mesenchymal and non-mesenchymal lineages; moreover, they are readily accessible and quickly proliferate in vitro, with lower senescence ratio than BM-MSC. In addition, the number of cells obtained by liposuction aspirates is usually sufficient for some clinical uses, avoiding further manipulation (17). Regarding their neural differentiation potential, we and others have recently demonstrated that A-MSC display a greater neuronal potential as compared to BM-MSC in vitro and after co-culture with Schwann cells (18–20).

Here we investigated the effect of brain-derived neurotrophic factor (BDNF) and retinoic acid (RA) on A-MSC. As shown on BM-MSC (21), we found evidence of long-lasting morphological, immunophenotypical and, most interestingly, electrophysiological changes of early neuronal differentiation.

Material and Methods

Isolation and culture of human A-MSC

Human A-MSC were obtained from 40 ml lipoaspirate samples of abdominal fat from female donors after

From the Departments of [1]Neurological Sciences and Vision, Section of Neurology, University of Verona, Verona; [2]Biology and Evolution, Section of Physiology and Biophysics - Stamina Group, University of Ferrara, Ferrara; [3]Morphological-Biomedical Sciences, Section of Anatomy, University of Verona, Verona; [4]Clinical and Experimental Medicine, Section of Haematology, University of Verona, Verona, Italy.

*These authors equally contributed to the work.

informed consent (22). Extracellular matrix was digested at 37°C in Hank's balanced salt solution with 1 mg/ml collagenase type I. Enzyme activity was neutralized with Dulbecco's modified Eagle medium (DMEM) containing 10% fetal bovine serum (FBS) (Gibco, Milan, Italy) and cells were centrifuged at 1200 g for 10 minutes; the pellet was then resuspended in 160 mM NH_4Cl to lyse contaminating red blood cells and filtered through a 70-µm nylon mesh. The cells were cultured at 30×10^6 cells/cm^2 in 25 cm^2 flasks in DMEM with high glucose concentration, GLUTAMAX I™, FBS, penicillin and streptomycin (all from Gibco). After 72 hours, non-adherent cells were removed. When 70–80% confluent, adherent cells were trypsinized, harvested and expanded in larger flasks. A homogenous cell population was obtained after 3 to 5 weeks of culture. All the experiments were performed at passages 7 to 16. Human A-MSC were characterized by the expression of CD105 (endoglin), CD73, CD29, CD44, CD90 class I HLA and lack of haematopoietic (CD45, CD14, CD34) and endothelial (CD31) markers. All the above monoclonal antibodies (mAb) were purchased from Pharmingen/Becton Dickinson. For immunophenotypical analysis, A-MSC were detached using trypsin/EDTA washed with PBS and resuspended at 10^6 cells/ml. Cell suspension was incubated in 15% FBS, followed by incubation with the specific mAb for 30 minutes. At least 10,000 events were analysed by flow cytometry (FACScalibur, Becton Dickinson) using Cell Quest software.

Neuronal differentiation protocol

Neuronal differentiation was induced by culturing A-MSC for 72 hours in serum-free medium with 20 ng/mL basic fibroblast growth factor (bFGF) and 20 ng/mL human epithelial growth factor (hEGF) (all from Peprotech), with the formation of floating bodies within 2–6 days. Such spheres were then subjected to immunocytochemistry or dissociated and seeded on poly-L-lysinated coverslips (Sigma Aldrich, Saint Louis, MO) at 1000/cm^2 in DMEM, 2% FBS, 10 ng/mL BDNF (Peprotech) and 0.75 mM all-trans RA (Sigma). Medium was replaced every 5–6 days up to 30 days, when the cells were subjected to morphological, immunocytochemical and electrophysiological analysis to assess the presence of neuronal features. Alternatively, neuronal induction medium was replaced with basal medium for 7 days and the stability of the neuronal features was assessed as above.

Cytochemistry and immunocytochemistry

Cellular morphology was evaluated at light microscope after fixation in 4% paraformaldehyde and hematoxilin staining or at scanning electron microscope (DSM 950, Zeiss, Germany) after sequential fixation in glutaraldehyde and 1% osmium tetroxide for 15 minutes, dehydration and final fixation with colloidal silver and gold. The immunophenotype of A-MSC was evaluated with antibodies directed against the mesenchymal marker CD105 (1:500, Caltag Laboratories, Burlingame, CA); the neuronal markers microtubule-associated protein 2 (MAP-2) and neuronal nuclear antigen (Neu-N) (both 1:1,000); nestin (1:200), a protein of intermediate filament expressed by neural stem cells; the oligodendroglial marker GalC (1:100) (all from Chemicon Inc., Temecula, CA), the astrocytic markers S-100 (1:5,000) and glial fibrillary acidic protein (GFAP) (1:10,000, Dako); tyroxine hydroxilase (TH), an enzyme of catecholaminergic neurons (1:2,000, Santa Cruz Biotechnolgy, Inc., Santa Cruz, USA); sodium channel (1:800) and α subunit of GABA-A receptor (1:400; Sigma). After washing, appropriate biotynilated secondary antibody and ABC amplification kit (Vector Laboratories, Burlingame, CA) were added and the reaction visualized with diaminobenzidine. Negative control included the omission of primary antibodies. Experiments were performed in triplicate and the percentage of positive cells was blindly calculated. To determine the mitotic activity of A-MSC before and after neural induction, cells were exposed to 10 µM BrdU (Sigma) for 4 hours, fixed with cold ethanol for 20 minutes, treated with 2N HCl and then with 0.1M NaBo, pH 9. Double immunofluorescence was performed for MAP-2 and BrdU, whose signals were detected with secondary antibodies conjugated respectively with Streptavidine Texas Red (Vector) and FITC (Boehringer, 1:10). Nuclei were stained with 50 µg/ml DAPI (Sigma). Cells were observed at the fluorescent microscope (Zeiss MC80) and the rate of mitotic activity was calculated dividing the number of BrdU-positive ($^+$)/MAP-2$^+$ cells and that of BrdU$^+$/MAP-2$^-$ elements by the total DAPI$^+$ cells.

Electrophysiology

Coverslips with A-MSC were placed in the recording chamber (1 cm^3 volume) and mounted on Olympus BX50WI microscope. The cells were perfused at the rate of 2 ml/min with artificial cerebro-spinal fluid with the following composition (mM): 125 NaCl, 2.5 KCl, 26 $NaHCO_3$, 1.25 NaH_2PO_4, 2 $CaCl_2$, 1 $MgCl_2$, and 15 glucose (all from Sigma). Saline was continuously bubbled with 95% O_2/5% CO_2; the osmolarity was adjusted at 305 mOsm with glucose. Cells were exposed to tetrodotoxin (TTX, 1 µM, Alomone, Jerusalem, Israel) or tetraethylammonium (TEA, 20mM, Sigma). The tight-seal whole-cell recording technique was used. Borosilicate glass pipettes (O.D. 1.5 mm; I.D. 0.86 mm; Hilenberg, Malsfeld, Germany) with internal filament were adopted for recordings. The pipettes had a tip resistance ranging from 4 to 6 MΩ when filled with these solutions. Seal resistance was always greater than 2 GΩ. The solution used for the recording pipette-filling solution contained (mM) 120 KCl, 10 NaCl, 2 $MgCl_2$, 0.5 $CaCl_2$, 5 EGTA, 10 HEPES, 2 Na-ATP, 10 glucose; the osmolarity was adjusted at 295 mOsm with glucose, and pH at 7.2 with KOH. Membrane currents were recorded and acquired with Axopatch 200A amplifier (Molecular Devices, Sunnyvale, CA). The series resistance was around 15 MΩ; 60–70% compensation of the series resistance was routinely used. Data acquisition was performed by a Pentium-based computer using 12 bit A/D-D/A converters (Digidata 1200B; Molecular Devices). Prior to acquisition, the signals were filtered at half the sampling frequency by a lowpass 4-pole Bessel filter and digitised with sample times ranging from 10 to 100 µs. Offline analysis was performed using version 10.1 of pClamp

(Molecular Devices). Data were expressed as mean ± SEM and were statistically analysed using Origin 7.5 software (OriginLab, Northampton, MA).

Statistical analysis

The results obtained by cytochemistry and electrophysiology in basal conditions and after neuronal induction were evaluated by Student's *t*-test and the difference was considered statistically significant when $p < 0.05$.

Results

In basal conditions, confluent A-MSC appeared as large and flat spindle-shaped elements (Fig. 1A) without expression of neuronal markers, with the ability to differentiate into adipocytes, chondrocytes and osteoblasts, as previously described (19, 20). As already reported for BM-MSC (21), in the presence of hEGF and bFGF, A-MSC formed spherical, floating aggregates within 2–6 days (Fig. 1B), which expressed nestin, NeuN, and MAP-2 (Fig. 1C), but not the glial markers GalC, GFAP and S-100 (Fig. 1D) as well as CD105 (data non shown).

After 30 days of cultures in the presence of BDNF and RA, two populations were clearly distinguishable based on morphological and immunophenotypical criteria; about half (56.81 ± 2.26%) of A-MSC showed a characteristic neuronal morphology with contracted cytoplasm, condensed nucleus and protrusion of two or three cellular processes (Fig. 1E): by immunocytochemistry, these cells expressed nestin (Fig. 1F) and the neuronal markers MAP-2 and NeuN (Figs. 1G, H). A very low proportion of these cells (about 1%) expressed also TH and GABA-A receptor (Figs. 1I, J), while we failed to detect immunoreactivity for the sodium channel. Interestingly, no signal for the glial markers S-100, GFAP, GalC was observed (Fig. 1K). The remaining A-MSC showed no apparent response to the differentiation protocol and remained large and flat, with abundant cytoplasm and did not expressed any neuronal markers. Exposure to the differentiation medium greatly reduced the proliferation rate of A-MSC. In fact, none of the A-MSC with neuronal morphology and MAP-2 staining showed incorporation of BrdU, while 5 ± 1.5% of MAP-2$^-$ A-MSC with basal morphology was BrdU$^+$ (as compared to 7.5 ± 2.5% of untreated cells). Morphological and immunophenotypical changes suggestive of neuronal differentiation persisted for at least seven days after the removal of differentiation medium (Figs. 1L, M). The formation of spherical, floating aggregates before the treatment with BDNF/RA was fundamental to obtain neuronal differentiation: in the absence of this step, A-MSC subjected to the differentiation protocol continued to proliferate and maintained the basal biological features (data not shown). We evaluated electrophysiological properties in basal condition and after neuronal differentiation using the patch clamp technique in whole-cell configuration. Focusing on treated A-MSC with neuronal morphology, we estimated the membrane potential under current-clamp conditions and the presence of voltage-gated channels in whole-cell voltage-clamp experiments. The resting membrane potential of A-MSC with neuronal morphology (−59.75 ± 5.41 mV, n = 12) was significantly more negative than that of basal A-MSC (−33.54 ± 3.1 mV, n = 26; p = 0.001 (Fig. 2). Although not statistically different, also the mean value of membrane capacitance for differentiated A-MSC was lower (62.70 ± 9.67 pF, n = 10) than basal A-MSC (87.5 ± 9.51 pF, n = 28). A large outward current was isolated after blockage of inward currents with TTX. Depolarising pulses ranging from −50 to +40 mV in 10 mV increments from the holding potentials of −70 mV evoked a family of non-inactivating currents (Figs. 3A, B), significantly larger in differentiated A-MSC as compared to basal condition: at + 40 mV the mean amplitudes were 522.86 ± 117 pA (n = 10) in differentiated cells *versus* 223.34 ± 37.55 pA (n = 19) in basal cells (p = 0.005) (Fig. 3C). Their selective block by a combination of TEA in the bath or equimolar ion substitution of K^+ with Cs^+ in the intracellular solution indicated that these currents were carried by potassium ions.

Differentiated A-MSC also exhibited a prominent inward current (Fig. 3D), which was virtually absent on basal cells. This was isolated by equimolar ion substitution of intracellular K+ with Cs^+, and was evoked by voltage steps ranging from −50 to +40 mV after a complete removal of inactivation with a 200 ms step at −120 mV. At 0 mV the mean peak amplitude was −185.09 ± 4.65 pA (n = 7) in differentiated cells *versus* 4.65 ± 4.65 pA, n = 28 in basal cells (Fig. 3F). For their fast inactivation and their sensitivity to TTX these currents were definitely mediated by classical voltage-dependent sodium channels. The kinetic of the sodium current has been studied in detail. The development of inactivation was studied with a series of depolarising steps to the fixed potential of 0 mV after 180 ms conditioning pulses between −120 mV and −40 mV (Figs. 3G, H). The half-inactivation was at the potential of −57.7 mV and the time constant for the development of inactivation was 2.46 + 0.13 ms at 0 mV (n = 7). The removal of inactivation was studied using the protocol shown in the inset of Fig. 3I: two consecutive depolarising pulses to 0 mV from different holding potentials (−100 mV for the case represented in Fig. 3I) were separated by an interval of variable length. The longer was the time spent at the holding potential between the two steps, the larger was the removal of inactivation and the amplitude of the current in response to the second depolarising step; the time constant for the removal of inactivation was 2.0 ms at −100 mV.

The sub-population of A-MSC that maintained basal morphology and immunophenotype after the neural induction exhibited electrophysiological features very similar to untreated A-MSC (data not shown).

Discussion

Aim of this study was to evaluate the potential of A-MSC to assume long-lasting and selective features typical of neuronal cells. We focused our attention on A-MSC because they can be obtained by less invasive procedure and cultured with a greater proliferation rate than BM-MSC (17, 22). As MSC derived from other sources, A-MSC can be induced to differentiate also in non-mesenchymal lineages. Very few studies have assessed the neuronal differentiation potential of A-MSC in response to chemical agents or growth factors.

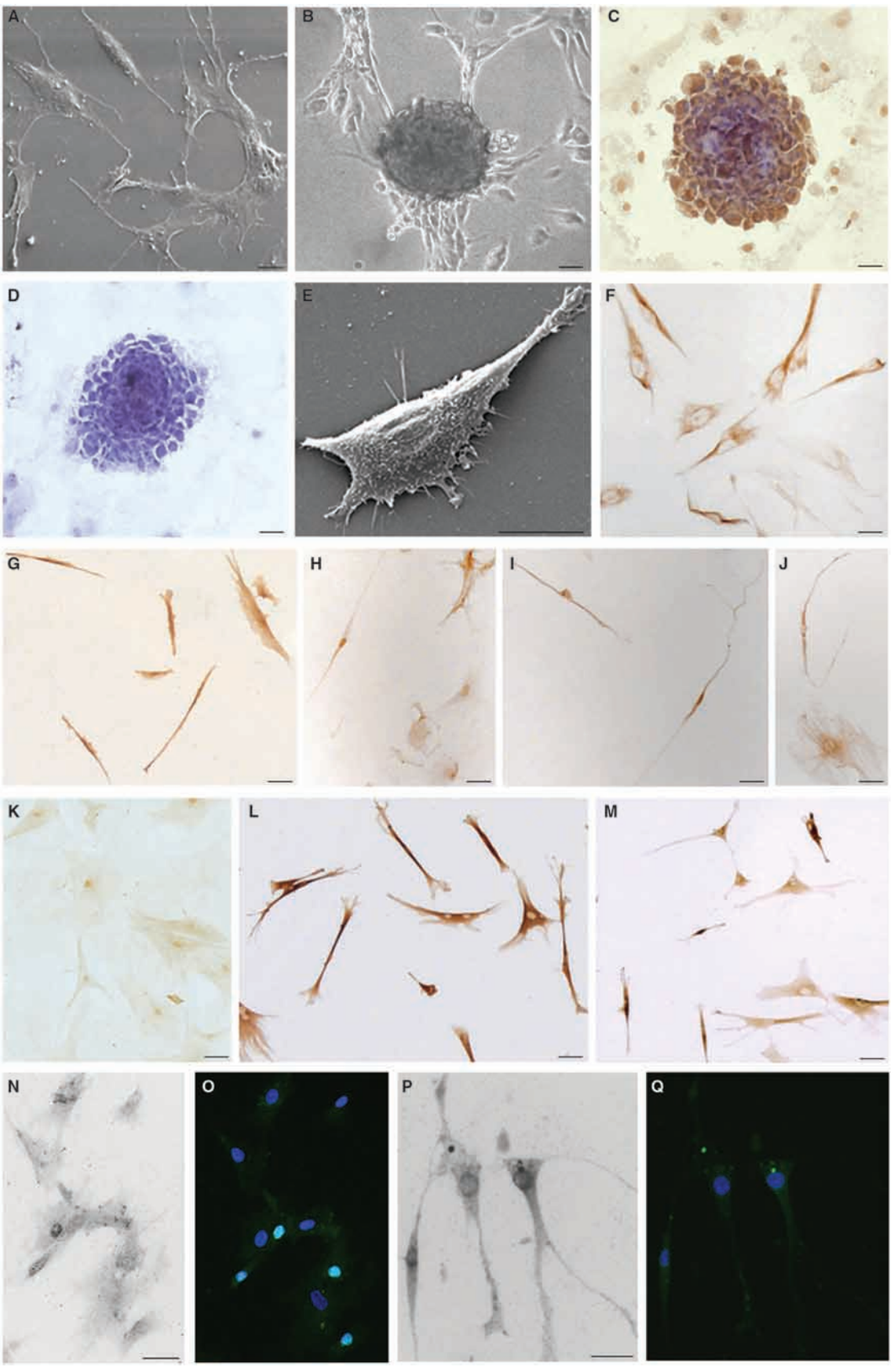
A
B
C
D
E
F
G
H
I
J
K
L
M
N
O
P
Q

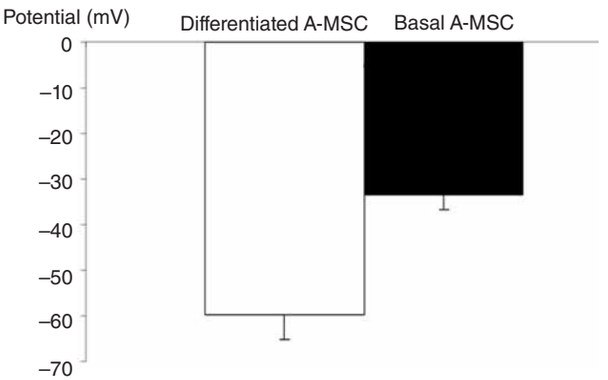

FIG. 2. Electrophysiological features of A-MSC subjected to neuronal differentiation. Values of resting membrane potential recorded in A-MSC in basal conditions and in A-MSC with neuronal morphology after exposure to neuronal differentiation protocol.

In addition, the data about the neuronal differentiation of A-MSC in terms of electrophysiological properties have provided not convincing results (23, 24), because of the use of chemical differentiation protocols, which promoted poorly specific neural changes with atypical morphological and electrophysiological profiles (25, 26). Interestingly, the comparison of neuronal differentiation of A-MSC and BM-MSC has recently suggested a higher potential of A-MSC, as compared to MSC from other sources. In this regard, we and others have found evidence that, in opportune culture conditions, A-MSC expressed higher levels of neuronal markers and responded to differentiation stimuli more promptly than BM-MSC (18–20).

In the present study the neuronal induction protocol included BDNF and RA, two factors already used to lead neuronal differentiation from neural stem cells (NSC) (27) and early neuronal functional profile or neurotransmettitor syntesis in MSC (21, 28, 29). The induction phase was preceded by the stimulation of A-MSC with mitogenic factors, in order to obtain high numbers of nestin-positive, floating spheres, very similar to the neurospheres derived from NSC (21). The subsequent exposure of A-MSC to RA and BDNF induced profound morphological, phenotypic and, more interestingly, electrophysiological changes suggestive of early neuronal differentiation. In fact, about 50% of A-MSC displayed morphological and immunocytochemical profile of neuronal cells, including the expression of TH and α subunit of GABA-A receptor in a small subset of differentiated cells. In addition, these A-MSC with neuronal features displayed resting membrane potential close to −60 mV, delayed-rectifier type K^+ currents, as well as voltage-dependent Na^+ currents, selectively inhibited by TTX, which in basal conditions were virtually absent. At variance with previous reports regarding BM-MSC (30–32), we and others have detected these features only after neuronal differentiation, but not in basal conditions or in A-MSC not responding to neural differentiating stimuli (14). The absence of immunoreactivity for Na^+ channel in differentiated A-MSC showing in-ward currents sensitive to TTX by patch-clamp is probably related to the different sensitivity between these two procedures, as already described (13).

Taken together, our results suggest that this protocol induced upon a high proportion of A-MSC early, though incomplete, neuronal differentiation. The possibility to obtain a full neuronal differentiation of MSC in vitro remains an intriguing challenge in the field of stem cells and central nervous system repair, particularly for neurodegenerative diseases. Cell-based therapy represents a promising tool, with NSC constituting the gold standard, because of high proliferation and neural differentiation potential. Apart from ethical considerations, allo-transplantation could limit the therapeutic efficacy (33–35), while auto-transplantation is largely limited by procedure invasiveness and their potential involvement in the disease (36, 37).

MSC can be a safe stem cell reserve and the BM-MSC transplantation was experimented in several neurological disease models, such as cerebral infarction (38), experimental autoimmune encephalomyelitis (39) and spinal cord injury (40) with beneficial therapeutic effects. In these experimental models, different mechanisms probably accounted for the neuroregenerative process, including activation of endogenous precursors by cell-to-cell contact and/or cytokine release, neuronal differentiation *in situ* and immunomodulation. Although the data about A-MSC are more limited, their therapeutic effects have been shown in the rat model of ischemic stroke and spinal cord injury (41, 42). Although studies in animal models of neurodegenerative diseases are needed to assess the function and safety of A-MSC in vivo, the ability of these cells to undergo neuronal differentiation in artificial sets indicates their potentiality to differentiate in the central nervous system microenvironment.

Acknowledgments

This work was in part funded by grants PRIN 2005, CARIVERONA 2005 to BB.

FIG. 1. Morphology and phenotype of A-MSC subjected to neuronal differentiation. (**A**) Morphology of A-MSC in basal condition at scanning electron microscope. Treatment with EGF and bFGF induced the formation of floating aggregates, formed by MAP-2-positive (**B**), GFAP-negative (**C**) elements. After exposure to RA and BDNF, A-MSC exhibited contracted cytoplasm and long processes at scanning electron microscope (**E**), expressed nestin (**F**) and the neuronal markers MAP-2 (**G**) and NeuN (**H**). A small portion of the differentiated A-MSC expressed TH (**I**) and α subunit of GABA-A receptor (**J**), but not the glial marker GFAP (**K**). Morphological and phenotypical changes persisted for at least 7 days, with expression of nestin (**L**) and MAP-2 (**M**). Bar: 50 μm.

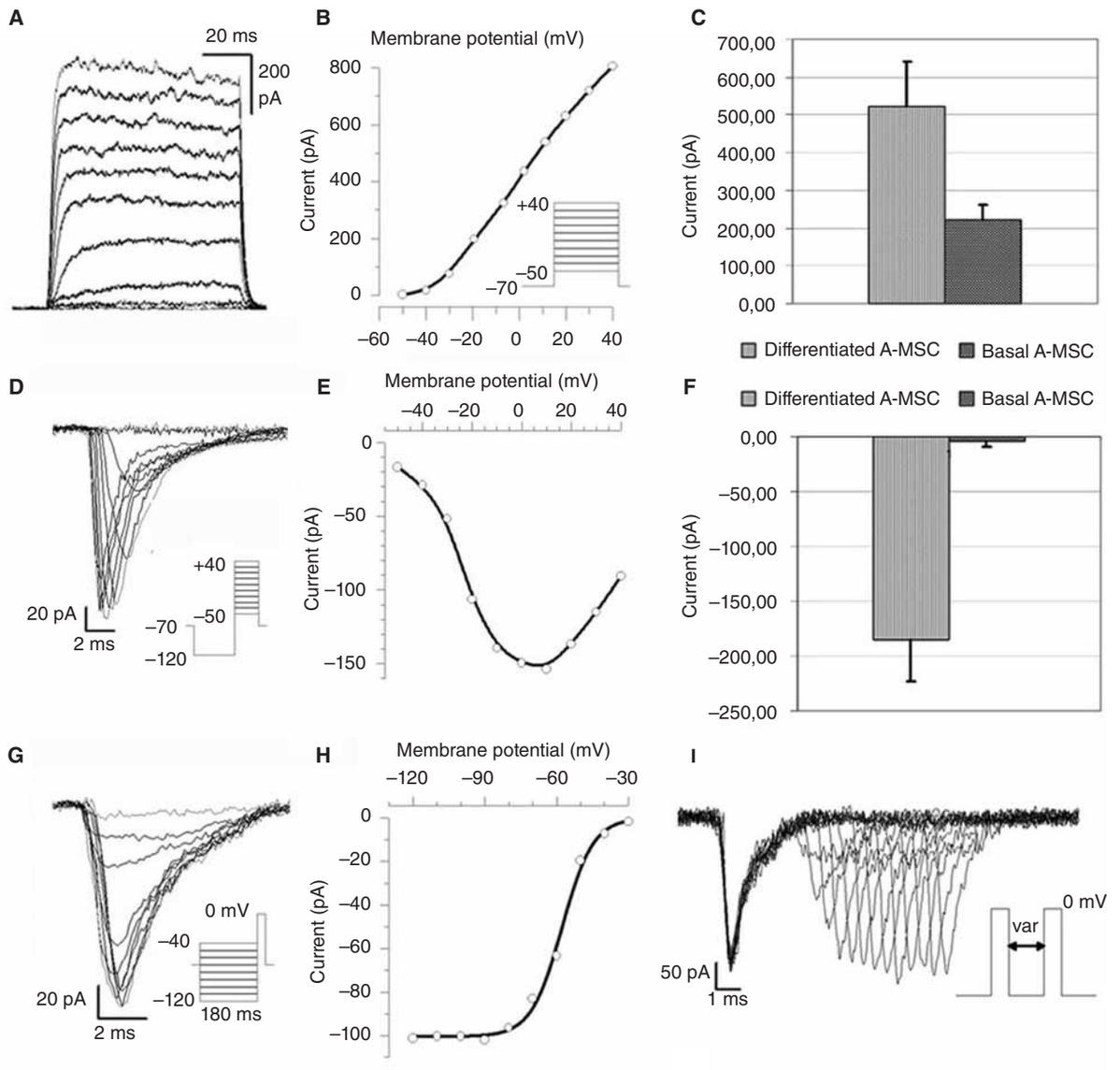

FIG. 3. Electrophysiological features of A-MSC subjected to neuronal differentiation. **A-B**: Activation of potassium currents evoked by depolarizing pulses ranging between −50 and + 40 mV and the corresponding current-voltage relationship in A-MSC with neuronal morphology (B). **C**: Voltage-clamp revealed a tendency for higher outward currents in differentiated A-MSC than in basal ones. **D-E**: Activation of sodium currents evoked by increasing depolarizing pulses as indicated in the inset and the corresponding current-voltage relationship in A-MSC with neuronal morphology (E). **F**: A-MSC with neuronal morphology exhibited inward currents significantly higher than basal cells. **G**, **H**: Inactivation of the sodium channels in A-MSC with neuronal morphology, obtained following the protocol shown in the inset. The corresponding current-voltage relationship (H), showing the peak amplitudes at the fixed test potential of 0 mV as a function of the conditioning pulse, has a midpoint centered at −57.7 mV. **I**: Removal of inactivation of the sodium current at −100 mV. Two pulses at 0 mV (inset) were separated by a variable delay to allow removal of inactivation, occurring in this case with a time constant of 2.0 ms.

References

1. Friedenstein AJ, RK Chailakhyan, NV Latsinik, AF Panasyuk, and IV Keiliss-Borok. (1974). Stromal cells responsable for transferring the microenvironment of the hemopoietic tissues. Transpl 17:331–340.
2. Noth U, AM Osyczka, R Tuli, NJ Hickok, KG Danielson and RS Tuan. (2002). Multilineage mesenchymal differentiation potential of human trabecolar bone-derived cells. J Orthop Res 20:1060–1069.
3. Da Silva Meirelles L, PC Chagastelles and NB Nardi. (2006). Mesenchymal stem cells reside in virtually all post-natal organs and tissue. J Cell Science 119:2204–2213.

4. Pittenger MF, AM Mackay, SC Beck, RK Jaiswal, R Douglas, JD Mosca, MA Moorman, DW Simonetti, S Craig and DR Marshak. (1999). Multilineare potential of adult human mesenchymal stem cells. Science 284:143–147.
5. Sanchez-Ramos J, S Song, F Cardozo-Pelaez, C Hazzi, T Stedeford, A Willing, TB Freeman, S Saporta, W Janssen, N Patel, DR Copper and PR Sanberg. (2000). Adult bone marrow stromal cells differentiate into neural cells in vitro. Exp Neurol 164:247–256.
6. Grove JE, E Bruscia and DS Krause. (2004). Plasticity of bone marrow-derived stem cells. Stem Cells 22:487–500.
7. Petersen BE, WC Bowen, KD Patrene, WM Mars, AK Sullivan, N Murase, SS Boggs, JS Greenberger and JP Goff. (1999). Bone marrow as a potential source of hepatic oval cells. Science 284:1168–70.
8. Jiang Y, BN Jahagirdar, RL Reinhardt, RE Schwartz, CD Keene, XR Ortiz-Gonzalez, M Reyes, T Lenvik, T Lund, M Blackstad, J Du, S Aldrich, A Lisberg, WC Low, DA Largaespada and CM Verfaillie. (2002). Pluripotency of mesenchymal stem cell derived from adult marrow. Nature 418:41–49.
9. Woodbury D, EJ Schwarz, DJ Prockop and IB Black. (2000). Adult rat and human bone marrow stem cells differentiate into neurons. J Neurosci Res 61:364–370.
10. Woodbury D, K Reynolds and IB Black. (2002). Adult bone marrow stem cells express germline, ectodermal, entodermal, and mesodermal genes prior to neurogenesis. J Neurosci Res 96: 908–917.
11. Lu P, A Blesch and MH Tuszynski. (2004). Induction of bone marrow stem cells to neurons: differentiation, trandifferentiation, or artifact? J Neurosci Res 77:174–191.
12. Croft AP and SA Przyborski. (2006). Formation of neurons by non-neural adult stem cells: potential mechanism implicates an artifact of growth in culture. Stem Cells 24:1841–1851.
13. Dezawa M, H Kanno, M Hoshino, H Cho, N Matsumoto, Y Itokazu, N Tajima, H Yamada, H Sawada, H Ishikawa, T Mimura, M Kitada, Y Suzuki and C Ide. (2004). Specific induction of neuronal cells from bone marrow stromal cells and application for autologous transplantation. J Clin Invest 113:1701–1710.
14. Egusa H, FE Schweizer, CC Wang, Y Matsuka, and J Nishimura. (2005). Neuronal differentiation of bone marrow-derived stromal stem cells involves suppression of discordant phenotypes through gene silencing. J Biol Chem 280:23691–23697.
15. Jiang Y, D Henderson, M Blackstad, A Chen, RF Miller, and CM Verfaillie. (2003). Neuroectodermal differentiation from a mouse multipotent adult progenitor cells. Proc Natl Acad Sci USA 100:11854–11860.
16. Wislet-Gendebien S, G Hans, P Leprince, JM Rigo, G Moonen, and B Rogister. (2005). Plasticity of cultured mesenchymal stem cells: switch from nestin-positive in excitable neuron-like phenotype. Stem Cells 23:392–402.
17. Kern S, H Eichler, J Stoeve,H Kluter and K Bieback. (2006). Comparative analysis of mesenchymal stem cells from bone marrow, umbelical cord blood or adipose tissue. Stem Cells 24:1294–1301.
18. Kang SK, LA Putnam, J Ylostalo, IR Popescu, J Dufour, A Belousov and BA Bunnell. (2004). Neurogenesis of rhesus adipose stromal cells. J Cell Sci 117:4289–4299.
19. Krampera M, S Marconi, A Pasini, M Galie, G Rigotti, F Mosna, M Tinelli, L L Lovato, E Anghileri, A Andreini, G Pizzolo, A Sbarbati and B Bonetti. (2007). Induction of neural-like differentation in human mesenchymal stem cells derived from bone marrow, flat, spleen and tymus. Bone 40:382–390.
20. Krampera M, S Sartoris, F Liotta, A Pasini, R Angeli, A Andreini, F Mosna, M Tinelli, B Bonetti, E Rebellato, MG Testi, F Frosali, G Pizzolo, G Tridente, E Maggi, S Romagnani and F Annunziato. (2007). Immune regulation by mesenchymal stem cells derived from adult spleen and thymus. Stem Cells Dev, in press.
21. Hermann A, R Gasti, S Liebau, MO Popa, J Fiedler, BO Boehm, M Maisel, H Lerche, J Schwarz, R Brenner and A Storch. (2004). Efficient generation of NSC-like cells from adult bone marrow stem cells. J Cell Sci 117:4411–4422.
22. Katz AJ, A Tholpady, SS Tholpady, H Shang, and RC Ogle. (2005). Cell surface and trascriptional characterization of human adipose-derived adherent stromal cells. Stem Cells 23:412–418.
23. Ashjian PH, AS Elbarbary, B Edmonds, D DeUgarte, M Zhu, PA Zuk, HP Lorenz, P Benhaim, and MH Hedrick. (2003). In vitro differentiation of human processed lipoaspirate cells into early neural progenitor. Plast Reconstr Surg 111:1922–1931.
24. Ning H, G Lin, TF Lue and CS Lin. (2006). Neuron-like differentiation of adipose tissue-derived stromal cells and vascular smooth muscle cells. Differentiation 74:510–518.
25. Hung SC, H Cheng, CY Pan, MJ Tsai, LS Kao and HL Ma. (2002). In vitro differentiation of size-sieved stem cells into electrically active neural cells. Stem Cells 20:522–529.
26. Safford KM, SD Safford, JM Gimble, AK Shetty and HE Rice. (2004). Characterization of neuronal/glial differentiation of murine adipose-derived adult stromal cells. Exp Neurol 187:319–328.
27. Jacobs S, DC Lie, KL DeCicco, Y Shi, LM DeLuca, FH Gage, and RM Evans. (2006). Retinoic acid is required early during adult neurogenesis in the dentate gyrus. Proc Natl. Acad Sci USA 103:3902–3907.
28. Zhao LX, J Zhang, F Cao, L Meng, DM Wang, YH Li, X Nan, WC Jiao, M Zheng, XH Xu, and XT Pei. (2004). Modification of the BDNF gene: a portal to transform mesenchymal stem cells into advantageous engineering cells for neurodegeneration and neuroprotection. Exp Neurol 190:396–406.
29. Kohyama J, H Abe, T Shimazaki, K Nakashima, S Gojo, T Taga, H Okano, J Hata and A Umezawa. (2001). Brain from bone: efficient meta-differentiation of marrow stroma-derived mature osteoblasts to neurons with noggin or a demethylating agent. Differentiation 68:235–244.
30. Heubach JF, EM Graf, J Leutheuser, M Bock, B Balana, I Zahanich, T Christ, S Boxberger, E Wettwer and U Ravens. (2004). Electrophysiological properties of human mesenchymal stem cells. J Physiol 554:659–672.
31. Li GR, H Sun, X Deng and CP Lau. (2005). Characterization of ionic current in human mesenchymal stem cells from bone marrow. Stem Cells 23:371–382.
32. Li GR, XL Deng, H Sun, SS Chung, HF Tse and CP Lau. (2006). Ion channels in mesenchymal stem cells from rat bone marrow. Stem Cells 24:1519–1528.
33. Rossi F and E Cattaneo. (2002). Neural stem cell therapy for neurological diseases: dreams and reality. Nat Rev 3:401–408.
34. Conti L, T Cataudella and E Cattaneo. (2003). Neural stem cells: a pharmacological tool for brain diseases? Pharm Research 47: 289–297.
35. Muraoka K, T Shingo, T Yasuhara, M Kameda, W Yuan, H Hayase, T Matsui, Y Miyoshi and I Date. (2006). The high integration and differentiation potential of autologous neural stem cells transplantation comparated with allogenic transplantation in adult rat hippocampus. Exp Neurol 199:311–327.
36. Hoglinger GU, P Rizk, MP Muriel, C Duyckaerts, WH Oertel, I Caille and EC Hirsch. (2004). Dopamine depletion impairs precursor cell proliferation in Parkinson disease. Nat Neurosci 7:726–735.
37. Liu Z and LJ Martin. (2006). The adult neural stem and progenitor cell niche is altered in amyotrophic lateral sclerosis mouse brain. J Comp Neurol 497:468–488.

38. Zhao LR, WM Duan, M Reyes, CD Keene, CM Verfaillie and WC Low. (2002). Human bone marrow stem cells exhibit neural phenotypes and ameliorate neurological deficits after grafting into the ischemic brain of rats. Exp Neurol 174:11–20.
39. Zappia E, S Casazza, E Pedemonte, F Benvenuto, I Bonanni, E Gerdoni, D Giunti, A Ceravolo, F Cazzanti, F Frassoni, G Mancardi and A Uccelli. (2005). Mesenchymal stem cells ameliorate experimental autoimmune encephalomyelitis inducing T-cell anergy. Blood 106:1755–1761.
40. Urdzakova L, P Jendelova, K Glogarova, M Burian, M Hajek and E Sykova. (2006). Transplantation of bone marrow stem cells as well as mobilization by granulocyte-colony stimulating factor promotes recovery after spinal cord injury in rats. J Neurotrauma 23:1379–1391.
41. Kang SK, DH Lee, YC Bae, HK Kim, SY Baik and JS Jung. (2003). Improvement of neurological deficits by intracerebral transplant of human adipose-derived stem cells after ischemia in rats. Exp Neurol 183:355–366.
42. Kang SK, MJ Shin, JS Jung, YG Kim and CH Kim. (2006). Autologous adipose tissue-derived stromal cells for treatment of spinal cord injury. Stem Cells Dev 15:583–594.

Address reprint requests to:
Dr. Bruno Bonetti, MD, PhD
Department of Neurological Sciences and Vision,
Section of Neurology,
University of Verona,
Ospedale Policlinico G.B. Rossi,
P. le Scuro 10,
37134 Verona, Italy

Phone: +39 045 8124694
Fax: +39 045 585933
E-mail: bruno.bonetti@univr.it

PE

AQ: Please provide volume number.
PE: Please provide manuscript history details.